EFDA–JET–CP(14)03/16

A. Huber, M. Wischmeier, C.G. Lowry, S. Brezinsek, C.F. Maggi, M.L. Reinke, G. Sergienko, L. Aho-Mantila, G. Arnoux, M.N.A. Beurskens, M. Clever, S. Devaux, H.G. Esser, C. Giroud, M. Groth, S. Jachmich, A. Järvinen, Ch. Linsmeier, B. Lipschultz, G.F. Matthews, G. Maddison, S. Marsen, A.G. Meigs, Ph. Mertens, M.F.F. Nave, V. Philipps, M. Stamp, S. Wiesen and JET EFDA contributors

Impact of Strong Impurity Seeding on the Radiation Losses in JET with ITER-Like Wall

Impact of Strong Impurity Seeding on the Radiation Losses in JET with ITER-Like Wall

A. Huber[1], M. Wischmeier[2], C.G. Lowry[3], S. Brezinsek[1], C.F. Maggi[2], M.L. Reinke[4], G. Sergienko[1], L. Aho-Mantila[5], G. Arnoux[3], M.N.A. Beurskens[3], M. Clever[1], S. Devaux[3], H.G. Esser[1], C. Giroud[3], M. Groth[6], S. Jachmich[7], A. Järvinen[6], Ch. Linsmeier[1], B. Lipschultz[4], G.F. Matthews[3], G. Maddison[3], S. Marsen[8], A.G. Meigs[3], Ph. Mertens[1], M.F.F. Nave[9], V. Philipps[1], M. Stamp[3], S. Wiesen[1] and JET EFDA contributors*

JET-EFDA, Culham Science Centre, OX14 3DB, Abingdon, UK

[1]Institute of Energy and Climate Research (Plasma Physics), Forschungszentrum Jülich, Germany
[2]MPI für Plasmaphysik, D-85748 Garching, Germany
[3]CCFE/Fusion Association, Culham Science Centre, Abingdon, OX14 3DB, UK
[4]University of York, Heslington, York, YO10 5DD, United Kingdom
[5]VTT Technical Research Centre of Finland, FI-02044 VTT, Finland
[6]Aalto University, Tekes, P.O.Box 4100, 02015 Espoo, Finland
[7]Laboratory for Plasma Physics, ERM/KMS, B-1000 Brussels, Belgium
[8]MPI für Plasmaphysik, D-17491 Greifswald, Germany
[9]Inst. de Plasmas e Fusão Nuclear, IST, Univ. de Lisboa, Lisbon, Portugal
** See annex of F. Romanelli et al, "Overview of JET Results", (24th IAEA Fusion Energy Conference, San Diego, USA (2012)).*

Preprint of Paper to be submitted for publication in Proceedings of the
41st EPS Conference on Plasma Physics, Berlin, Germany
23rd June 2014 – 27th June 2014

INTRODUCTION

Development of high radiation plasma scenarios with impurity seeding is necessary for the operation of burning plasma fusion devices with a reactor-relevant size such as DEMO, which should operate at high heating power and radiation fractions close to 95% [1].

Dedicated H-mode impurity seeding experiments with both strike points on the lower vertical targets have been performed during the last JET campaigns with ITER-like wall. The main objective of these experiments was to extend impurity seeding to the highest radiation fraction independently of the confinement mode and with various impurity species (N_2, Ne and Ar) and input heating powers. The impact of impurity seeding on the energy confinement has been studied as well as its dependence on the balance between main chamber and divertor radiation. Type I H-mode characteristics at $B_T = 2.7T$, $I_p = 2.5MA$ ($q_{95} = 3.3$) and Greenwald density fraction up to 85% in low-triangularity magnetic equilibria ($\delta = 0.22$) have been examined. Respective scans over a deuterium fuelling range of 2×10^{22} el/s ÷ 6.5×10^{22}el/s and an impurity seeding range of 2×10^{22} el/s ÷ 1.3×10^{23}el/s with an additional NBI-power of 18MW have been performed. Stable highly radiative discharges are obtained with feed-forward impurity seeding. Over the full range the power loss ($P_{loss} = P_{in}$-dW/dt) remains above the H-mode threshold according to the empirical scaling [2]. However, this scaling has been derived from the plasma pulses with $\gamma_{rad} = P_{rad}^{tot}/P_{heat} \leq 50\%$ and it is aim of these experiments to investigate whether this empirical scaling is relevant for highly radiative discharges with impurity seedings.

In Figure 1 two pulses with (red coloured) and without (blue coloured) nitrogen seeding at JET-ILW are compared. Both plasmas were heated with ≈ 18MW NBI in the same divertor magnetic configuration. The deuterium fuelling waveforms as well as the puffing locations (into inner and outer divertor scrape-off layer (SOL)) were identical during the first half of the pulses (fuelling rate of $\Gamma_{D2} \approx 4 \times 10^{22}$el/s). The BeII fast emission signal ($\lambda = 527nm$) in the outer divertor represents the ELMs behaviour. In contrast to an unseeded plasma, the N_2 seeding into the private flux of the outer divertor leg with $\Gamma_{N2} \approx 13.4 \times 10^{22}$ el/s demonstrates directly after the L-H transition small energy ELMs with a quick transition at 10.7s from a type I ELMy to an ELM-free H-mode phase with cold pedestal ($T_e^{ped} \approx 300eV$) with some recovery of the energy confinement. Such ELMy-free H-modes, called M-mode, accompanied by coherent magnetic oscillations have been observed in [3] at heating powers just above the threshold for L-H transitions. In the unseeded plasma the global confinement was generally degraded at increasing fuelling levels to reach the high density close to Greenwald limit [4]. The seeding of N_2 leads to higher Z_{eff} which increases during the seeding by ≈50% (increase of $\Delta Z_{eff} = 0.6$) in comparison with the unseeded pulse. At 12s the total radiative power reaches its peak-value (≈ 75%). Most of the radiation originates from the X-point region in this detached case as the tomographic reconstructions show (figure 2d). The nitrogen seeding causes a considerable energy confinement recovery from a confinement factor of $H_{98Y} = 0.65$ in the pulse with D_2 fuelling only to a factor of $H_{98Y} = 0.75$ in the N_2 case: The profiles of electron temperature T_e and electron density n_e at the outer mid-plane around the edge barrier were

measured by the High Resolution Thomson Scattering system [5]. They show a significant impact of the N_2 seeding. In contrast to the unseeded plasma, the n_e profile in the N_2 seeded pulse becomes more peaked (see Figure 1b): n_e increases in the plasma core and decreases in the edge region correspondingly. At the same time T_e rises across the entire profile with N_2 seeding. Therefore, the seeding significantly affects particle confinement and transport, thus possibly increasing the energy stored in the plasma. The confinement improvement during the N_2 seeding in JET-ILW has been recently reported in [6].

Figure 2 shows the radiation distributions for the seeding range from $\Gamma_{N2} \approx 2 \times 10^{22}$el/s to $\Gamma_{N2} \approx 1.3 \times 10^{23}$el/s. Up to $\Gamma_{N2} \approx 4 \times 10^{22}$el/s, a significant radiation is observed in the vinicity of the X-point as well as in the inner and outer SOL with the presence of small Type I ELMs for the entire duration of the seeding. Beyond $\Gamma_{N2} \approx 6 \times 10^{22}$ el/s the radiation "spills over" into the region above the X-point inside of the separatrix. Nitrogen seeding at a maximum rate of $\Gamma_{N2} \approx 1.3 \times 10^{23}$el/s leads to stable and steady state ELM free H-mode (or M-mode) with radiation fraction of $\gamma_{rad} \sim 75\%$.

Figure 3 shows the radiation distribution in the main chamber versus divertor region with various injected impurity species (N_2, Ne and Ar). The divertor radiation P_{div} is defined as the radiation emitted below $Z \leq -1.0$m, and $P_{rad}^{bulk} = P_{rad}^{tot} - P_{rad}^{div.}$ The observed divertor radiation fraction ($\gamma_{rad}^{div} = P_{rad}^{div}/P_{rad}^{tot}$) is highest for low-Z seeding gases. The spatial distribution of radiation, as well as γ_{rad}^{div}, does not show a clear dependance on D_2-fueling in N_2-seeded, type-I ELMy H-mode pulses. The maximal value of $\gamma_{rad}^{div} \sim 70\%$ in N_2 seeded pulses was found at $f_{rad} \sim 60\%$. The confinement increases from $H_{98Y} = 0.6$ in unseeded pulses with $\gamma_{rad} \sim 30\%$ to a value of $H_{98Y} = 0.75$ at $\gamma_{rad} \sim 50\%$. Further increase of γ_{rad} leads to a moderate confinement degradation. Beyond $\gamma_{rad} \sim 55\%$, the energy confinement scaling factor remains almost constant at ≈ 0.7.

Argon and neon seeding further increased the fraction of the total radiation up to 63% which is below that of the highest nitrogen cases of 75% The radiation distribution became slightly more biased towards the core with contribution of about half of radiation fraction in the divertor region ($\gamma_{rad}^{div} \approx 0.5$), as one might expect from the temperature dependence of the radiative loss cooling function [7]. In contrast to nitrogen seeding which causes a considerable improvement of the energy confinement, the Ar injection causes only a moderate one. Seeding with Ar leads to an H-L transition with γ_{rad} of ~ 60% just prior to the H-L switchover.

The neon seeded discharges showed beyond $\gamma_{rad} \sim 50\%$ a ELM-free phase (or M-mode) with a sequence of H-L-H transitions, as shown in details in Figure 4. During transient L-mode periods of these transitions, the radiated power fraction increases up to 95%, while the density is decreasing in the core and in the edge. The radiation profiles show completely different behaviours during the transition cycles as shown in Figure 4: L-mode period – radiation pattern around the X-point with strong contribution in the outer and inner SOL; H-mode period (or M-mode) – radiation is peaked in the region above the X-point inside the separatrix. Improvement of the confinement factor up to $H_{98Y} \approx 0.75$ at $\gamma_{rad} \sim 50\%$ (see figure 3) was observed with Ne seeding during the

ELM-free H-mode (or M-mode) phases. The Z_{eff} is increasing for the duration of the seeding by ≈ 80% (increase of $\Delta Z_{eff} = 0.9$).

Power load mitigation and divertor detachment at both target plates have been observed with all seeding gases. Under cold detached divertor, the tungsten cannot significantly contribute to the total radiation. The radiation is almost entirely from the seeded impurities.

The maximum of the radiation fraction of $\gamma_{rad} \sim 75\%$ have been achieved with N_2 seeding. It has not yet been determined whether this is the limit of what can be achieved, but the increase of the radiation fraction has become an increasingly weak function of the seeding rate. Further investigations are required before drawing irrevocable conclusions.

ACKNOWLEDGEMENTS.

This work was supported by EURATOM and carried out within the framework of the European Fusion Development Agreement. The views and opinions expressed herein do not necessarily reflect those of the European Commission.

REFERENCES

[1]. N. Asakura et al., Journal of Plasma and Fusion Research SERIES, **9** (2010)
[2]. Y. Martin et al. 2008 Journal of Physics: Conference Series 123012033
[3]. E.R. Solano et al., 40th EPS Conference., Finland, 2013P4.111
[4]. A. Huber et al., Journal of Nuclear Materials **438** (2013), S139
[5]. R. Pasqualotto et al., Review of Scientific Instruments **75** (2004) 3891
[6]. C. Giroud et al., Nuclear Fusion **53** (2013) 113025
[7]. http://www.adas.ac.uk

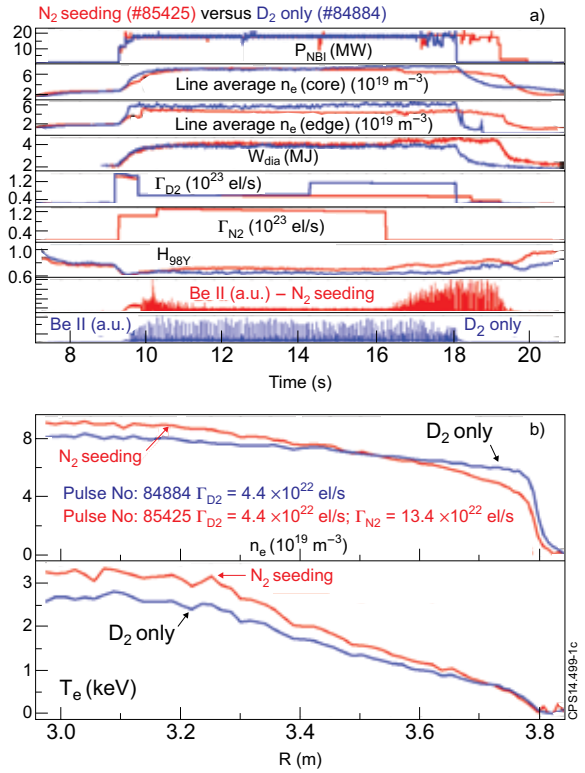

Figure 1: Comparison between nitrogen seeded plasma (red) and plasma pulse fuelled with D_2 only: time traces (a) and ne and T_e profiles (b).

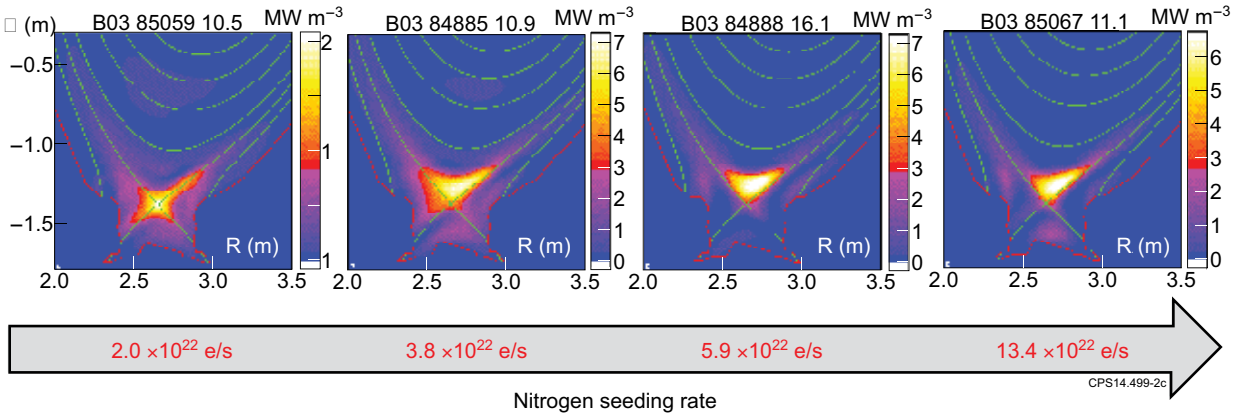

Figure 2: Radiation distribution in the divertor for N_2 seeded plasma with different level of the seeding rate.

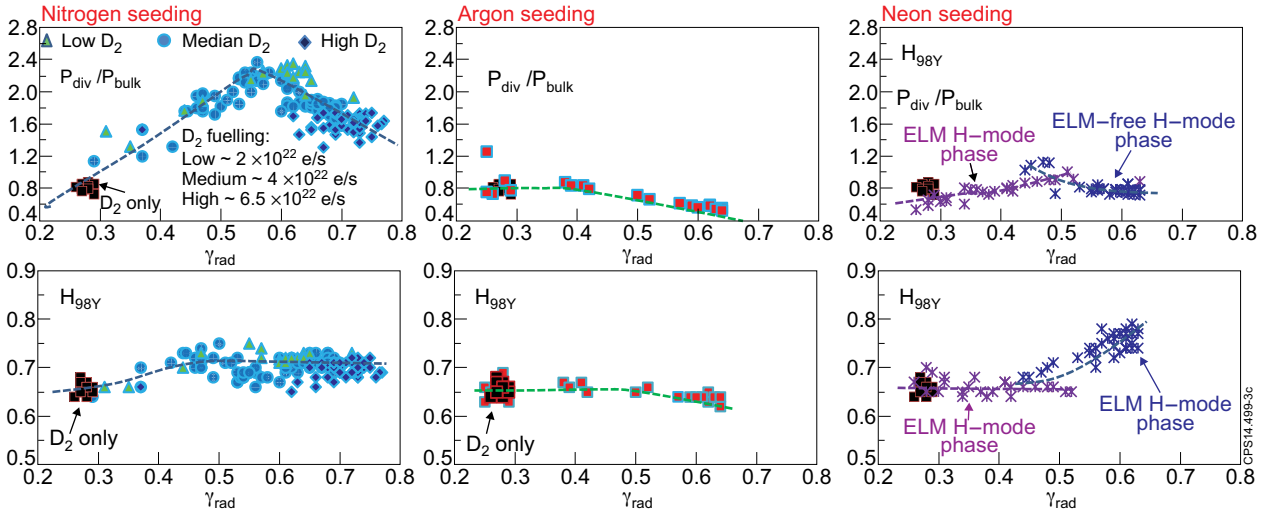

Figure 3: Radiation distribution in the main chamber versus divertor region.

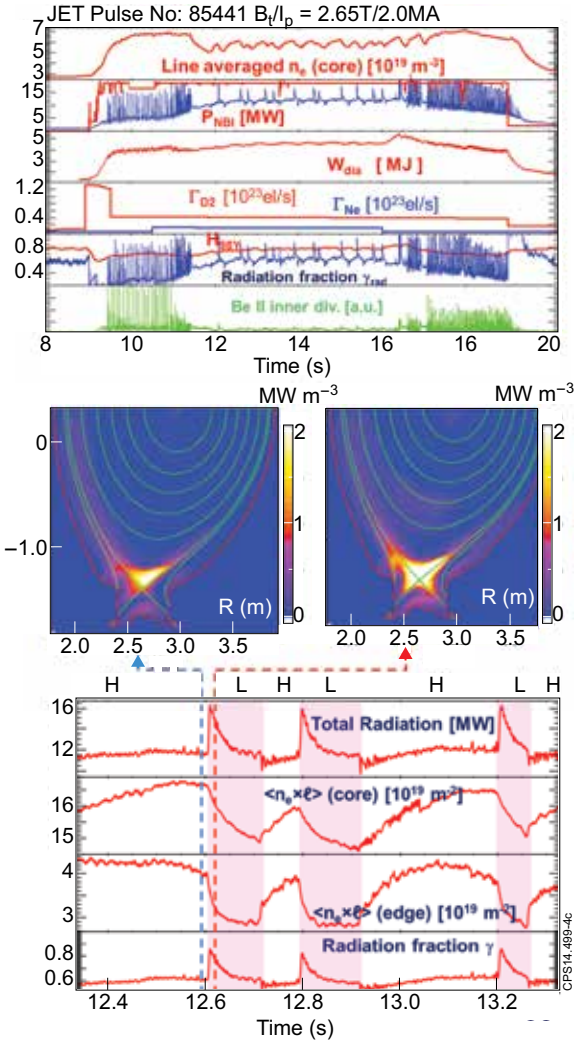

Figure 4: Sequence of H-L-H confinement transitions (dithering cycles) during the neon seeding. Tomographic reconstructions of the total radiation during the different phases of the transitions.